Journal of Materials Chemistry C

ROYAL SOCIETY OF CHEMISTRY

PAPER

View Article Online
View Journal | View Issue

Cite this: J. Mater. Chem. C, 2022, 10, 5489

Achieving 17.5% efficiency for polymer solar cells *via* a donor and acceptor layered optimization strategy†

Wenjing Xu,[a] Xiong Li,[b]* Sang Young Jeong,[c] Jae Hoon Son,[c] Zhengji Zhou,[d]* Qiuju Jiang,[e] Han Young Woo,[c] Qinghe Wu,[e] Xixiang Zhu,[a] Xiaoling Ma[a] and Fujun Zhang[a]*

Received 3rd January 2022,
Accepted 1st March 2022

DOI: 10.1039/d2tc00024e

rsc.li/materials-c

Layer-by-layer polymer solar cells (LbL-PSCs) were prepared with PNTB6-Cl as the donor and Y6 as the acceptor by a sequential spin-coating method. Two solvent additives DPE and DFB were individually incorporated into PNTB6-Cl chlorobenzene solution and Y6 chloroform solution. A PCE of 17.53% was achieved for the optimal LbL-PSCs with two solvent additives, which is much larger than the PCE of 16.38% for the LbL-PSCs without solvent additives. Over 7% PCE enhancement can be realized by individually employing solvent additives in donor and acceptor layers, resulting from the simultaneously enhanced open circuit voltage (V_{OC}) of 0.88 V, short circuit current density (J_{SC}) of 26.63 mA cm^{-2} and fill factor (FF) of 74.83%. The photogenerated exciton distribution, charge transport and collection in the LbL-PSCs can be optimized by employing different solvent additives in donor and acceptor solutions. Meanwhile, the efficient energy transfer from PNTB6-Cl to Y6 can provide an additional channel for improving the exciton utilization efficiency through exciton dissociation at PNTB6-Cl/Y6 interfaces. Meanwhile, the PCEs of LbL-PSCs are better than those of bulk heterojunction PSCs with the same materials and solvent additives, indicating the great potential of LbL-PSCs for commercial application.

Introduction

The power conversion efficiencies (PCEs) of bulk heterojunction polymer solar cells (BHJ-PSCs) have markedly increased in the recent years due to the rapid development of novel donor and acceptor materials, interfacial materials and device engineering.[1–5] Incorporation of additives has been commonly confirmed as an efficient route to optimize the phase separation degree for achieving efficient PSCs.[6–8] The excellent compatibility of the used materials is considered as the prerequisite to form a bi-continuous interpenetrating network for preparing efficient BHJ-PSCs.[9–12] Very recently, LbL-PSCs were prepared by a sequential spin-coating method, exhibiting comparable or slightly higher PCEs in comparison with the corresponding BHJ-PSCs of the same materials.[13–19] The underlying reasons for LbL-PSCs being highly efficient are needed to be clarified for better understanding the dynamic process in the LbL active layers. It is well known that the exciton diffusion distance is about 20 nm in organic semiconducting materials, and the BHJ structure can provide sufficient donor/acceptor interfaces for exciton dissociation within a short diffusion distance.[20] In the LbL-PSCs, donor and acceptor interfacial penetration may provide an additional interface for exciton dissociation, as reported in previous reports.[21,22] The thickness of donor layers are more than 50 nm in the LbL-PSCs, donor/acceptor interfacial penetration may take limited function for improving the exciton dissociation in LbL-PSCs. It is well known that most of the excitons will be generated near the ITO electrode according to the Beer–Lambert principle when the sun light is illuminated from the glass substrate.[23–26] The energy transfer from the donor to the acceptor may provide a vital channel to fully make use of photogenerated excitons near the ITO electrode. The excitons on acceptors close to the donor/acceptor interface, generated by energy transfer from the donor, will be easily

[a] Key Laboratory of Luminescence and Optical Information, Ministry of Education, Beijing Jiaotong University, 100044, Beijing, China. E-mail: fjzhang@bjtu.edu.cn
[b] Department of Physics, Beijing Technology and Business University, 100048, Beijing, China. E-mail: lixiong@btbu.edu.cn
[c] Organic Optoelectronic Materials Laboratory, Department of Chemistry, College of Science, Korea University, 02841, Seoul, Republic of Korea
[d] Key Lab for Special Functional Materials, Ministry of Education, National and Local Joint Engineering Research Center for High-Efficiency Display and Lighting Technology, and School of Materials, Henan University, 475004, Kaifeng, Henan Province, China. E-mail: zzj@henu.edu.cn
[e] Department of Chemistry and Key Laboratory for Preparation and Application of Ordered Structural Materials of Guangdong, Shantou University, 515063, Guangdong, China

† Electronic supplementary information (ESI) available. See DOI: 10.1039/d2tc00024e

dissociated into free charge carriers for improving the PCE of LbL-PSCs. The efficient energy transfer from the donor to the acceptor may be a prerequisite to select materials for preparing highly efficient LbL-PSCs.[27,28]

In this work, a series of LbL-PSCs and BHJ-PSCs were prepared by employing PNTB6-Cl as the donor and Y6 as the acceptor based on the normal structures of ITO/PEDOT:PSS/PNTB6-Cl/Y6/PNDIT-F3N/Ag and ITO/PEDOT:PSS/PNTB6-Cl:Y6/PNDIT-F3N/Ag, respectively. The solvent additives DPE with a boiling point (BP) of 259 °C and DFB with a BP of 90.4 °C were selected to optimize the molecular arrangement in BHJ and LbL active layers. The DPE was incorporated into PNTB6-Cl in chlorobenzene solution and DFB was incorporated into Y6 in chloroform solution for optimizing the donor and acceptor layers, respectively. The PNTB6-Cl chain arrangement should be optimized during the DPE slow volatilization process. The DFB with a low BP will suffer a rapid volatilization to adjust a small molecular acceptor arrangement, leading to more efficient electron transport channels, which can be confirmed from the enhanced FF of PSCs with solvent additives. The chemical structures of used materials are exhibited in Fig. 1a. The PNTB6-Cl film can be kept well while spin-coating Y6 solution on it because the polymer PNTB6-Cl is hardly dissolved in chloroform.[29] The absorption spectra of LbL films without or with solvent additives were measured and are shown in Fig. 1b. The refractive index (n) and extinction coefficient (k) of LbL films were measured to investigate the effect of solvent additives on the photogenerated exciton distribution and are exhibited in Fig. 1c. The n and k of LbL films are slightly increased by incorporating appropriate solvent additives, indicating the enhanced photon harvesting ability of LbL films due to the optimized molecular arrangement. The optimal LbL-PSCs exhibit a PCE of 17.53%, benefiting from the simultaneously enhanced open circuit voltage (V_{OC}) of 0.88 V, short circuit current density (J_{SC}) of 26.63 mA cm^{-2} and fill factor (FF) of 74.83%. The PCE of the optimal LbL-PSCs is much larger than 16.38%, 16.61% and 16.65% obtained for the LbL-PSCs without and with DPE or DFB as the solvent additive, which should result from the enhanced photon harvesting and well optimized molecular arrangement in the PNTB6-Cl and Y6 layers. More than 7% PCE improvement can be achieved by employing the two solvent additive strategy, benefiting from the individually layered optimization on donor and acceptor layers. Although the PCEs of BHJ-PSCs are slightly increased from 14.46% to 14.81% by incorporating DPE and DFB solvent additives in the blended chlorobenzene solutions, they are still much lower than 17.53% for the optimized LbL-PSCs.

Experimental results

The current density *versus* applied voltage (J–V) curves of LbL-PSCs and the typical BHJ-PSCs were measured under one

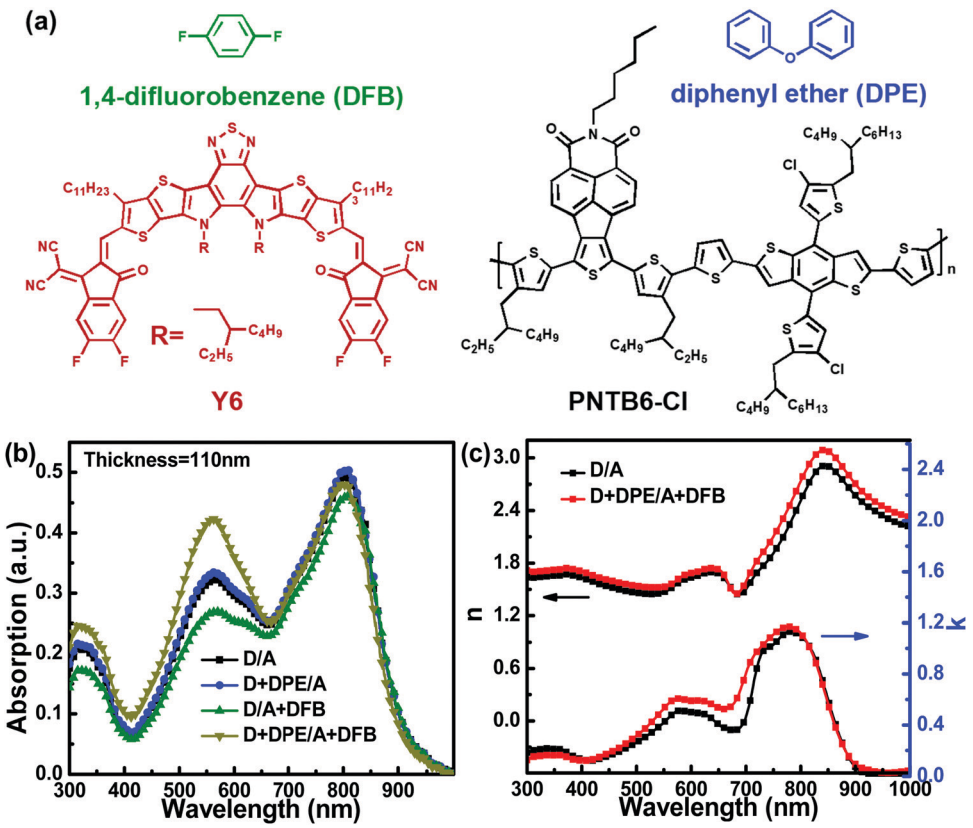

Fig. 1 Chemical structures of (a) Y6, DFB, PNTB6-Cl and DPE. (b) The absorption spectra of PNTB6-Cl/Y6 films without or with solvent additives. (c) The n and k curves of PNTB6-Cl/Y6 films without or with solvent additives.

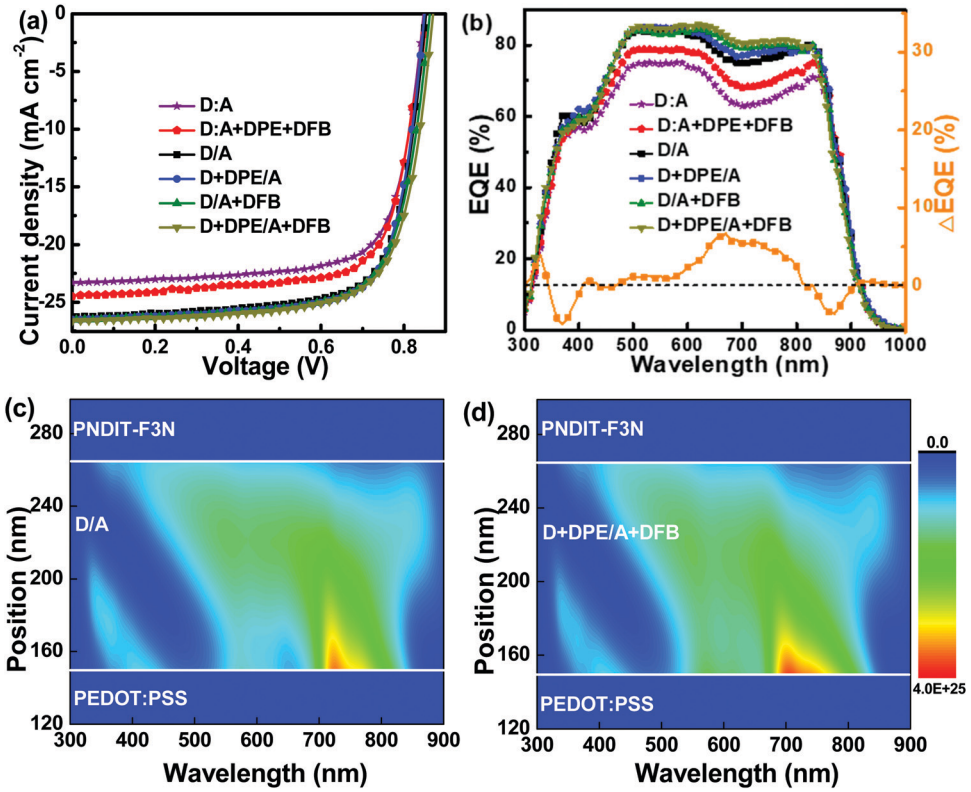

Fig. 2 BHJ and LbL-PSCs prepared without or with solvent additives: (a) The *J*–*V* curves, (b) the EQE spectra and the ΔEQE between the additive-processed LbL devices and the control one. (c) Photogenerated exciton distribution in PNTB6-Cl/Y6 layers, and (d) photogenerated exciton distribution in PNTB6-Cl + DPE/Y6 + DFB layers.

standard simulated solar light illumination and are exhibited in Fig. 2a. Obviously, the solvent additives DPE and DFB have a positive effect on the performance of PSCs from comparatively analyzing the photovoltaic parameters. The PCEs of LbL-PSCs can be improved from a PCE of 16.38% for the cells without any solvent additive to 16.61% or 16.65% by individually employing the DPE or the DFB solvent additive. The PCE of the optimal LbL-PSCs is markedly increased to 17.53% by individually incorporating solvent additives in donor and acceptor solutions, benefiting from the simultaneously enhanced V_{OC} of 0.88 V, J_{SC} of 26.63 mA cm^{-2} and FF of 74.83%. More than 7% PCE improvement is obtained *via* using double solvent additives for the layered optimization on donor and acceptor layers. The PCEs of BHJ-PSCs can be slightly improved from 14.46% to 14.81% by employing DPE and DFB as solvent additives, resulting from the increased FFs and J_{SC}s. The series resistance (R_S) and shunt resistance (R_{SH}) are calculated according to the *J*-*V* curves of LbL-PSCs and the typical BHJ-PSCs. It is apparent that the R_S values of LbL-PSCs are slightly lower than those of BHJ-PSCs and R_{SH} values of LbL-PSCs are slightly larger than those of BHJ-PSCs, indicating the more efficient charge transport in the LbL active layers. Meanwhile, solvent additives play a vital role in decreasing R_S and increasing R_{SH}, leading to the FF increase of PSCs with solvent additives. The minimum R_S of 1.24 Ω cm^2 and maximum R_{SH} of 399 Ω cm^2 were obtained for the LbL-PSCs with double additives, which are responsible for the highest FF of LbL-PSCs with double additives. The detailed photovoltaic parameters of all LbL-PSCs and BHJ-PSCs are summarized in Table 1. The EQE spectra of LbL-PSCs and BHJ-PSCs were measured and are exhibited in Fig. 2b. The EQE difference (ΔEQE) between the

Table 1 Photovoltaic parameters of PSCs without or with solvent additives

Structure	Active layer	J_{SC} (mA cm^{-2})	*Cal.* J_{SC} (mA cm^{-2})	V_{OC} (V)	FF (%)	PCE (Ave. ± Dev.) (%)	R_S [Ω cm^2]	R_{SH} [Ω cm^2]
BHJ	D:A	23.29	22.87	0.85	72.08	14.46 (14.35 ± 0.12)	2.06	237
	D:A + DPE + DFB	23.78	23.56	0.85	73.28	14.81 (14.68 ± 0.13)	2.01	267
LbL	D/A	26.29	25.26	0.85	73.25	16.36 (16.23 ± 0.14)	1.80	342
	D + DPE/A	26.53	25.39	0.85	73.64	16.61 (16.53 ± 0.17)	1.38	359
	D/A + DFB	26.51	25.31	0.87	72.16	16.65 (16.47 ± 0.15)	1.81	340
	D + DPE/A + DFB	26.63	25.64	0.88	74.83	17.53 (17.34 ± 0.19)	1.24	399

The average and deviation of PCEs were calculated from 10 individual cells.

LbL-PSCs without additives and the optimized LbL-PSCs was calculated and is shown in Fig. 2b. It is apparent that the ΔEQE values are larger than zero in the spectral range from 410 nm to 800 nm, which can well support the increased J_{SC} of PSCs with two additives. The integral area between the ΔEQE curve and the ΔEQE = 0 line is about 8.9, and the positive integral area further indicates increased photon utilization efficiency in the optimal LbL-PSCs. To further clarify the positive effect of solvent additives on the performance improvement of PSCs, the photogenerated exciton distribution in the LbL active layers was calculated by using the transfer matrix method.[30] The detailed calculation process is described in the supporting information. The photogenerated exciton distribution in the LbL active layers without or with solvent additives is exhibited in Fig. 2c and d. The distinct photogenerated exciton distribution can be observed in the LbL active layers due to the effect of solvent additives on the n and k values of active layers, as well as the interference between the incident light and the reflected light from the Ag electrode.[31,32] In the whole spectral range from 300 nm to 900 nm, the photon generation rate is increased from 6.676×10^{29} to 6.715×10^{29} m^{-3} s^{-1} by employing two solvent additives, indicating the enhanced photon harvesting ability in the LbL active layers processed with two solvent additives.

To further investigate the underlying reason for PCE improvement of LbL-PSCs by solvent additives, the J–V curves of all LbL-PSCs were measured in the dark and one standard simulated solar light illumination under bias; the photogenerated current density (J_{PH}) is equal to the photocurrent density (J_L) minus dark current density (J_D), expressed as $J_{PH} = J_L - J_D$. The effective voltage (V_{eff}) is defined as the voltage at $J_{PH} = 0$ minus the applied bias. The J_{PH} *versus* effective bias (J_{PH}–V_{eff}) curves of all LbL-PSCs were measured and are exhibited in Fig. 3a. The photogenerated current density of LbL-PSCs can be defined as J_{PH}^*, $J_{PH}^{\&}$ and J_{SAT} under the short-circuit condition, the maximal output-power condition and the saturated state condition, respectively. The exciton dissociation efficiency (η_D) and charge collection efficiency (η_C) can be well evaluated from the ratios of J_{PH}^*/J_{SAT} and $J_{PH}^{\&}/J_{SAT}$, respectively.[33,34] The detailed values of all LbL-PSCs are listed in Table 2. The η_D and η_C of the optimal LbL-PSCs are 96.69% and 86.34%, which are larger than 95.57% and 82.32% for the LbL-PSCs without any solvent additive. The enhanced η_D and η_C can well support the PCE improvement in optimal LbL-PSCs. The J_{PH} of LbL-PSCs can rapidly arrive at the saturated states, also indicating the more efficient charge collection in LbL active layers processed with solvent additives. The exciton dynamic process between PNTB6-Cl and Y6 was investigated according to the photoluminescence (PL) spectra of neat and layer-by-layer films without or with solvent additives, and the corresponding PL spectra are shown in Fig. 3b. It is apparent that PL emission of PNTB6-Cl can be sufficiently quenched in the PNTB6-Cl/Y6 layer, indicating efficient exciton dissociation or energy transfer from PNTB6-Cl to Y6. The apparent spectral overlap between the PL spectrum of PNTB6-Cl and the absorption spectrum of Y6 can be observed from the image of Fig. 3b,

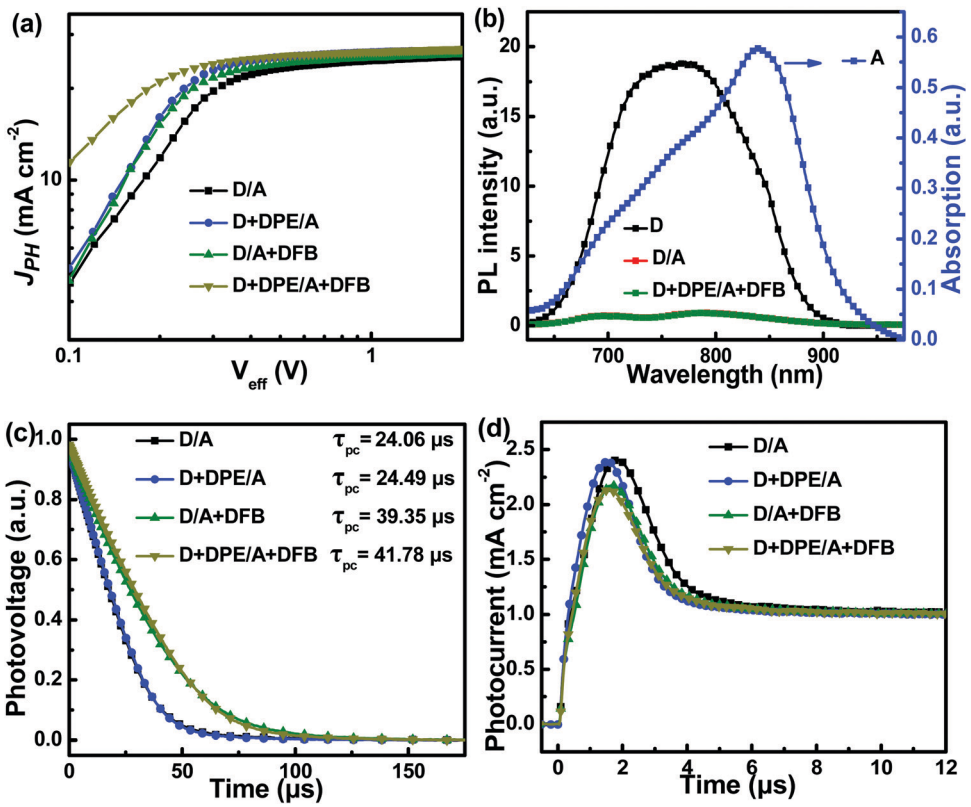

Fig. 3 (a) J_{PH}–V_{eff} curves of LbL-PSCs without or with solvent additives, (b) PL spectra of the pure PNTB6-Cl film, PNTB6-Cl/Y6 films without or with solvent additives and the absorption spectrum of the pure Y6 film, (c) Transient photovoltage curves and (d) photo-CELIV curves of all LbL-PSCs.

Table 2 The key parameters of LbL-PSCs without or with additives

Active layer	J_{SAT} (mA cm^{-2})	J_{PH}^{*} (mA cm^{-2})	$J_{PH}^{\&}$ (mA cm^{-2})	η_D (%)	η_C (%)
D/A	27.52	26.30	22.65	95.57	82.32
D + DPE/A	27.63	26.53	22.95	96.02	83.06
D/A + DFB	27.59	26.51	22.93	96.09	83.10
D + DPE/A + DFB	27.82	26.87	24.02	96.69	86.34

suggesting the efficient energy transfer from PNTB6-Cl to Y6 according to the FÖrster energy principle.[35–38] The photogenerated excitons on PNTB6-Cl near the ITO electrode can transfer their energy to Y6; the excitons generated *via* energy transfer on Y6 near PNTB6-Cl/Y6 interfaces will be dissociated into free charge carriers. The efficient energy transfer from PNTB6-Cl to Y6 will provide another channel for improving the PCE of LbL-PSCs.

Transient photovoltage (TPV) is a convenient method to analyze the charge recombination degree in PSCs by evaluating the photocarrier lifetime (τ_{pc}) under open-circuit conditions.[39–41] The TPV curves of all LbL-PSCs were measured under a white LED with a light intensity of 720 W m^{-2} and are shown in Fig. 3c. The τ_{pc} in the optimal LbL-PSCs is about 41.78 μs, which is much longer than 24.06 μs in LbL-PSCs without solvent additives, 24.49 μs in LbL-PSCs with the solvent additive DPE and 39.35 μs in LbL-PSCs with the solvent additive DFB. The prolonged τ_{pc} in the optimal LbL-PSCs further proves the weakest charge recombination, which should be beneficial to charge transport and collection in the corresponding LbL-PSCs. Under a short circuit condition, the transient photocurrent (TPC) of all LbL-PSCs were measured to obtain the charge extraction time (τ_{ext}).[42–45] The TPC curves of all LbL-PSCs are exhibited in Fig. S2 (ESI†). The τ_{ext} in optimal LbL-PSCs is about 0.207 μs, which is much shorter than 0.285 μs in LbL-PSCs without solvent additives, 0.239 μs in LbL-PSCs with the solvent additive DPE and 0.220 μs in LbL-PSCs with the solvent additive DFB. The relatively short τ_{ext} in the optimal LbL-PSCs reveals that the appropriate solvent additives can enhance charge transport and collection in the corresponding LbL-PSCs. It is well known that charge carrier mobility (μ) will directly influence charge transport and recombination in the active layers, which can be estimated from the photo-CELIV measurements.[46–48] The photo-CELIV curves of all LbL-PSCs were measured under a white LED with light intensity of 720 W m^{-2} and are exhibited in Fig. 3d. The charge mobility in the LbL active layers can be estimated based on the following equation: $\mu = \frac{2d^2}{3At_{max}^2\left[1+0.36\frac{\Delta j}{j_{(0)}}\right]}\left(\text{if } \Delta j < j_{(0)}\right)$, where d is the active layer thickness, A is the ramp rate, t_{max} is the time when the extracted current reaches its maximum value, $j_{(0)}$ represents the dark capacitive current, and Δj is the transient current peak height. The factor $1 + 0.36\ \Delta j/j_{(0)}$ in the formula is an empirical correction accounting for the redistribution of the electric field. As seen from Fig. 3d, the relatively small Δj is conducive to obtaining a large μ in the optimal LbL-PSCs. The calculated μ in the optimal LbL-PSCs is about 1.843×10^{-4} cm^2 V^{-1} s^{-1}, which is larger than 1.428×10^{-4} cm^2 V^{-1} s^{-1} in LbL-PSCs without solvent additives, 1.584×10^{-4} cm^2 V^{-1} s^{-1} in LbL-PSCs with the solvent additive DPE and 1.755×10^{-4} cm^2 V^{-1} s^{-1} in LbL-PSCs with the solvent additive DFB. The enhanced μ in LbL-PSCs should be beneficial to suppress charge recombination and improve charge collection, resulting in the relatively large FF of 74.83% for the optimal LbL-PSCs. The space charge limited current (SCLC) model was further employed to investigate hole mobility (μ_h) and electron mobility (μ_e) values based on the hole-only and electron-only devices.[49–51] The detailed $\ln(JL^3/V^2)$ *versus* $(V/L)^{0.5}$ curves of hole-only and electron-only devices are exhibited in Fig. S3 (ESI†); the μ_h, μ_e and μ_h/μ_e in the LbL active layers without or with solvent additives are summarized in Table 3. It is apparent that the μ_h and μ_e in the LbL active layers can be slightly increased by incorporating appropriate solvent additives. The μ_h/μ_e in the LbL active layers with two solvent additives is closest to 1, indicating the more balanced hole and electron mobility as confirmed from the relatively large FF of 74.83% in the optimal LbL-PSCs.[52]

To investigate the effects of solvent additives on the morphology, AFM was employed to characterize morphology of the neat and layer-by-layer films without or with solvent additives, as exhibited in Fig. S4 (ESI†). It is apparent that the root-mean-square (RMS) roughness of neat and layer-by-layer films can be slightly increased by incorporation of solvent additives, and the detailed RMS values are listed in the corresponding AFM images. The enhanced RMS of PNTB6-Cl with the DPE layer may be conducive to enlarging PNTB6-Cl/Y6 interfaces for exciton dissociation.[53] The AFM images of PNTB6-Cl + DPE/Y6 + DFB and PNTB6-Cl/Y6 films are exhibited in Fig. 4a. The RMS values of LbL films are increased from 0.618 nm to 0.702 nm by incorporation of solvent additives, which may result from the molecular crystallization induced by solvent additives.[54,55] GIWAXS characterization was carried out to further investigate molecular crystallization induced by solvent additives. The 2D-GIWAXS images and the corresponding out-of-plane (OOP) and in-plane (IP) profiles of PNTB6-Cl + DPE/Y6 + DFB and PNTB6-Cl/Y6 films are displayed in Fig. 4b and c. The PNTB6-Cl/Y6 films exhibit a lamellar stacking peak at 0.28 Å^{-1} in the IP direction and π–π stacking peak at 1.71 Å^{-1}

Table 3 The key parameters of LbL-PSCs without or with additives and the measured charge mobility according to the SCLC method

Active layer	TPV (μs)	TPC (μs)	μ (cm^{-2} V^{-1} s^{-1})	μ_h (cm^{-2} V^{-1} s^{-1})	μ_e (cm^{-2} V^{-1} s^{-1})	μ_h/μ_e
D/A	24.06	0.285	1.42×10^{-4}	4.15×10^{-4}	3.20×10^{-4}	1.30
D + DPE/A	24.49	0.239	1.58×10^{-4}	5.54×10^{-4}	4.50×10^{-4}	1.23
D/A + DFB	39.35	0.220	1.75×10^{-4}	7.16×10^{-4}	6.12×10^{-4}	1.17
D + DPE/A + DFB	41.78	0.207	1.84×10^{-4}	9.13×10^{-4}	8.52×10^{-4}	1.07

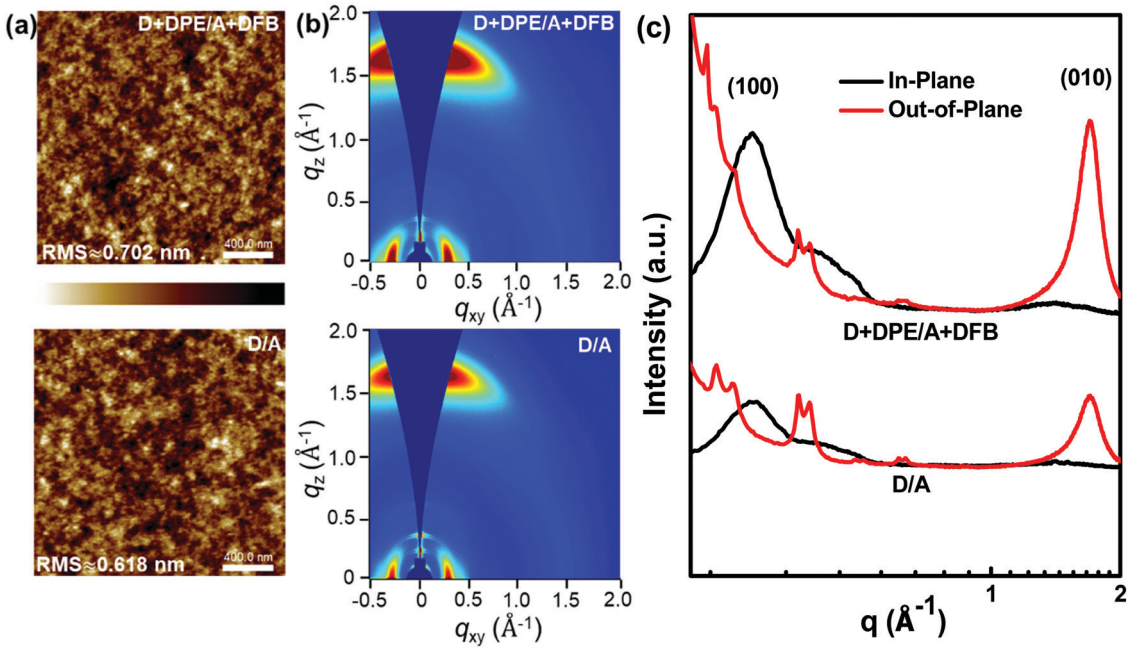

Fig. 4 The atomic force microscopy (AFM) images of (a) D + DPE/A + DFB and D/A layer-by-layer films. (b) 2D grazing-incidence wide-angle X-ray scattering (GIWAXS) patterns of D + DPE/A + DFB and D/A layer-by-layer films without or with solvent additives. (c) In-plane (black lines) and out-of-plane (red lines) line-cut profiles abstracted from the corresponding 2D GIWAXS images.

in the OOP direction, implying the existence of face-on molecular orientation in LbL films without solvent additives.[56–58] The OOP (010) and IP (100) diffraction peak intensity of the PNTB6-Cl + DPE/Y6 + DFB films are obviously enhanced by incorporation of solvent additives, indicating the more ordered face-on orientation in the LbL films. The improved molecular arrangement is beneficial to charge transport in the optimal LbL active layers, which can be confirmed from the relatively large μ_h and μ_e in comparison with the LbL active layers without solvent additives. The more ordered molecular arrangement in LbL active layers is conducive to charge transport and suppresses charge recombination, resulting from the enhanced performance of LbL-PSCs processed with two solvent additives.

Conclusions

In summary, BHJ and LbL-PSCs were fabricated with PNTB6-Cl as the donor and Y6 as the acceptor by employing a two solvent additive strategy. A PCE of 17.53% was achieved for the optimal LbL-PSCs, benefiting from the simultaneously enhanced V_{OC} of 0.88 V, J_{SC} of 26.63 mA cm^{-2} and FF of 74.83%. The molecular arrangement of PNTB6-Cl and Y6 can be individually optimized by appropriately incorporating DPE and DFB, as confirmed from the crystallinity and morphology of films without and with solvent additives. Over 7% PCE improvement can be achieved by employing a two solvent additive strategy in comparison with the LbL-PSCs without solvent additives. The 17.53% PCE of LbL-PSCs is much larger than 14.81% for the optimized BHJ-PSCs with the same materials and solvent additives, indicating that a deep understanding of the exciton dynamic process in LbL-PSCs is still needed. This work indicates the great potential of LbL-PSCs with excellent PCE for the commercial applications.

Author contributions

W. Xu and X. Ma carried out the device fabrication and characterization; F. Zhang, X. Li and Z. Zhou designed the experiments and finished the manuscript writing; Q. Jiang and Q. Wu synthesized the donor material PNTB6-Cl; X. Zhu also took part in the experiments; X. Ma, J. Son, S. Jeong and H. Woo carried out the GIWAXS experiment and analysis. All the authors discussed and commented on the paper.

Conflicts of interest

The authors declare no competing interests.

Acknowledgements

This work was supported by the National Natural Science Foundation of China (62175011, 61975006 and 62105017), the Postdoctoral Innovative Talent Support Program (BX20200042), the China Postdoctoral Science Foundation (2020M680327) and the Beijing Natural Science Foundation (4192049).

References

1 Y. Cui, Y. Xu, H. Yao, P. Bi, L. Hong, J. Zhang, Y. Zu, T. Zhang, J. Qin, J. Ren, Z. Chen, C. He, X. Hao, Z. Wei and J. Hou, *Adv. Mater.*, 2021, **33**, 2102420.

2 L. Hong, H. Yao, Y. Cui, P. Bi, T. Zhang, Y. Cheng, Y. Zu, J. Qin, R. Yu, Z. Ge and J. Hou, *Adv. Mater.*, 2021, **33**, 2103091.
3 Y. Lin, J. Wang, Z. Zhang, H. Bai, Y. Li, D. Zhu and X. Zhan, *Adv. Mater.*, 2015, **27**, 1170–1174.
4 C. Yan, S. Barlow, Z. Wang, H. Yan, A. Jen, S. Marder and X. Zhan, *Nat. Rev. Mater.*, 2018, **3**, 18003.
5 J. Wang and X. Zhan, *Acc. Chem. Res.*, 2021, **54**, 132–143.
6 X. Ma, A. Zeng, J. Gao, Z. Hu, C. Xu, J. H. Son, S. Y. Jeong, C. Zhang, M. Li, K. Wang, H. Yan, Z. Ma, Y. Wang, H. Y. Woo and F. Zhang, *Natl. Sci. Rev.*, 2021, **8**, nwaa305.
7 Y. Cai, Y. Li, R. Wang, H. Wu, Z. Chen, J. Zhang, Z. Ma, X. Hao, Y. Zhao, C. Zhang, F. Huang and Y. Sun, *Adv. Mater.*, 2021, **33**, 2101733.
8 Y. Zeng, D. Li, Z. Xiao, H. Wu, Z. Chen, T. Hao, S. Xiong, Z. Ma, H. Zhu, L. Ding and Q. Bao, *Adv. Energy Mater.*, 2021, **11**, 2101338.
9 W. Xu, X. Ma, J. Son, S. Jeong, L. Niu, C. Xu, S. Zhang, Z. Zhou, J. Gao, H. Woo, J. Zhang, J. Wang and F. Zhang, *Small*, 2022, **18**, 2104215.
10 L. Zhan, S. Li, T. Lau, Y. Cui, X. Lu, M. Shi, C. Li, H. Li, J. Hou and H. Chen, *Energy Environ. Sci.*, 2020, **13**, 635–645.
11 Z. Wang, X. Zhu, J. Zhang, K. Lu, J. Fang, Y. Zhang, Z. Wang, L. Zhu, W. Ma, Z. Shuai and Z. Wei, *J. Am. Chem. Soc.*, 2018, **140**, 1549–1556.
12 T. Xia, Y. Cai, H. Fu and Y. Sun, *Sci. China: Chem.*, 2019, **62**, 662–668.
13 J. Wan, L. Zhang, Q. He, S. Liu, B. Huang, L. Hu, W. Zhou and Y. Chen, *Adv. Funct. Mater.*, 2020, **30**, 1909760.
14 Y. Wang and X. Zhan, *Adv. Energy Mater.*, 2016, **6**, 1600414.
15 X. Zhang, Y. Li, D. Zhang, G. Wu, H. Zhang, J. Zhou, X. Li, Z. Saud, J. Zhang, Z. Wei, H. Zhou and Y. Zhang, *Sci. China: Chem.*, 2020, **64**, 116–126.
16 P. Cheng, R. Wang, J. Zhu, W. Huang, S. Chang, L. Meng, P. Sun, H. Cheng, M. Qin, C. Zhu, X. Zhan and Y. Yang, *Adv. Mater.*, 2018, **30**, 1705243.
17 H. Chen, T. Zhao, L. Li, P. Tan, H. Lai, Y. Zhu, X. Lai, L. Han, N. Zheng, L. Guo and F. He, *Adv. Mater.*, 2021, **33**, 2102778.
18 S. Park, S. Chandrabose, M. Price, H. Ryu, T. Lee, Y. Shin, Z. Wu, W. Lee, K. Chen, S. Dai, J. Zhu, P. Xue, X. Zhan, H. Woo, J. Kim and J. Hodgkiss, *Nano Energy*, 2021, **84**, 105924.
19 M. Nam, J. Na, J. Shin, H. Lee, R. Chang and D. Ko, *Nano Energy*, 2020, **74**, 104883.
20 L. Ye, Y. Xiong, Z. Chen, Q. Zhang, Z. Fei, R. Henry, M. Heeney, B. O'Connor, W. You and H. Ade, *Adv. Mater.*, 2019, **31**, 1808153.
21 H. Fu, W. Gao, Y. Li, F. Lin, X. Wu, J. Son, J. Luo, H. Woo, Z. Zhu and A. Jen, *Small Methods*, 2020, **4**, 2000687.
22 L. Zhan, S. Li, X. Xia, Y. Li, X. Lu, L. Zuo, M. Shi and H. Chen, *Adv. Mater.*, 2021, **33**, 2007231.
23 Z. Zhao, M. Liu, K. Yang, C. Xu, Y. Guan, X. Ma, J. Wang and F. Zhang, *Adv. Funct. Mater.*, 2021, **31**, 2106009.
24 M. Liu, J. Wang, K. Yang, Z. Zhao, Z. Zhou, Y. Ma, L. Shen, X. Ma and F. Zhang, *J. Mater. Chem. C*, 2021, **9**, 6357–6364.
25 R. Sun, J. Guo, C. Sun, T. Wang, Z. Luo, Z. Zhang, X. Jiao, W. Tang, C. Yang, Y. Li and J. Min, *Energy Environ. Sci.*, 2019, **12**, 384–395.
26 K. Yang, J. Wang, Z. Zhao, Y. Sun, M. Liu, Z. Zhou, X. Zhang and F. Zhang, *Chem. Eng. J.*, 2022, **435**, 134973.
27 T. Liu, X. Xue, L. Huo, X. Sun, Q. An, F. Zhang, T. P. Russell, F. Liu and Y. Sun, *Chem. Mater.*, 2017, **29**, 2914–2920.
28 X. Ma, W. Gao, J. Yu, Q. An, M. Zhang, Z. Hu, J. Wang, W. Tang, C. Yang and F. Zhang, *Energy Environ. Sci.*, 2018, **11**, 2134–2141.
29 H. Ning, Q. Jiang, P. Han, M. Lin, G. Zhang, J. Chen, H. Chen, S. Zeng, J. Gao, J. Liu, F. He and Q. Wu, *Energy Environ. Sci.*, 2021, **14**, 5919–5928.
30 R. Sun, Q. Wu, J. Guo, T. Wang, Y. Wu, B. Qiu, Z. Luo, W. Yang, Z. Hu, J. Guo, M. Shi, C. Yang, F. Huang, Y. Li and J. Min, *Joule*, 2020, **4**, 407–419.
31 K. Weng, L. Ye, L. Zhu, J. Xu, J. Zhou, X. Feng, G. Lu, S. Tan, F. Liu and Y. Sun, *Nat. Commun.*, 2020, **11**, 2855.
32 X. Ma, J. Wang, Q. An, J. Gao, Z. Hu, C. Xu, X. Zhang, Z. Liu and F. Zhang, *Nano Energy*, 2020, **70**, 104496.
33 G. Yuan, H. Fan, S. Wan, Z. Jiang, Y. Liu, K. Liu, H. Bai, X. Zhu and J. Wang, *J. Mater. Chem. A*, 2019, **7**, 20274–20284.
34 Z. Zhao, B. Liu, C. Xu, M. Liu, K. Yang, X. Zhang, Y. Xu, J. Zhang, W. Li and F. Zhang, *J. Mater. Chem. C*, 2021, **9**, 5349–5355.
35 K. Jiang, J. Zhang, Z. Peng, F. Lin, S. Wu, Z. Li, Y. Chen, H. Yan, H. Ade, Z. Zhu and A. Jen, *Nat. Commun.*, 2021, **12**, 468.
36 X. Ma, J. Wang, J. Gao, Z. Hu, C. Xu, X. Zhang and F. Zhang, *Adv. Energy Mater.*, 2020, **10**, 2001404.
37 Z. Hu, Z. Wang, Q. An and F. Zhang, *Sci. Bull.*, 2020, **65**, 131–137.
38 J. Gao, W. Gao, X. Ma, Z. Hu, C. Xu, X. Wang, Q. An, C. Yang, X. Zhang and F. Zhang, *Energy Environ. Sci.*, 2020, **13**, 958–967.
39 W. Gao, T. Liu, R. Sun, G. Zhang, Y. Xiao, R. Ma, C. Zhong, X. Lu, J. Min, H. Yan and C. Yang, *Adv. Sci.*, 2020, **7**, 1902657.
40 T. Dai, X. Li, Y. Zhang, D. Xu, A. Geng, J. Zhao and X. Chen, *Sol. Energy*, 2020, **201**, 330–338.
41 Z. Hu, J. Wang, Z. Wang, W. Gao, Q. An, M. Zhang, X. Ma, J. Wang, J. Miao, C. Yang and F. Zhang, *Nano Energy*, 2019, **55**, 424–432.
42 V. Le Corre, A. Chatri, N. Doumon and L. Koster, *Adv. Energy Mater.*, 2017, **7**, 1701138.
43 R. Wang, D. Zhang, S. Xie, J. Wang, Z. Zheng, D. Wei, X. Sun, H. Zhou and Y. Zhang, *Nano Energy*, 2018, **51**, 736–744.
44 M. Jiang, H. Bai, H. Zhi, J. Sun, J. Wang, F. Zhang and Q. An, *ACS Energy Lett.*, 2021, **6**, 2898–2906.
45 J. Seifter, Y. Sun and A. Heeger, *Adv. Mater.*, 2014, **26**, 2486–2493.
46 Y. Cui, H. Yao, J. Zhang, T. Zhang, Y. Wang, L. Hong, K. Xian, B. Xu, S. Zhang, J. Peng, Z. Wei, F. Gao and J. Hou, *Nat. Commun.*, 2019, **10**, 2515.
47 W. Lan, Y. Liu, B. Wu, B. Xu, H. Pu, B. Wei, Y. Peng, W. Tian and F. Zhu, *ACS Appl. Energy Mater.*, 2019, **2**, 7385–7392.
48 X. Ma, C. Tang, Y. Ma, X. Zhu, J. Wang, J. Gao, C. Xu, Y. Wang, J. Zhang, Q. Zheng and F. Zhang, *ACS Appl. Mater. Interfaces*, 2021, **13**, 57684–57692.

49 X. Xu, L. Yu, H. Meng, L. Dai, H. Yan, R. Li and Q. Peng, *Adv. Funct. Mater.*, 2021, **31**, 2108797.
50 Y. Lin, Y. Firdaus, M. Nugraha, F. Liu, S. Karuthedath, A. Emwas, W. Zhang, A. Seitkhan, M. Neophytou, H. Faber, E. Yengel, I. McCulloch, L. Tsetseris, F. Laquai and T. Anthopoulos, *Adv. Sci.*, 2020, **7**, 1903419.
51 W. Gao, Q. An, M. Hao, R. Sun, J. Yuan, F. Zhang, W. Ma, J. Min and C. Yang, *Adv. Funct. Mater.*, 2020, **30**, 1908336.
52 C. Xu, K. Jin, Z. Xiao, Z. Zhao, X. Ma, X. Wang, J. Li, W. Xu, S. Zhang, L. Ding and F. Zhang, *Adv. Funct. Mater.*, 2021, **31**, 2107934.
53 X. Wang, L. Zhang, L. Hu, Z. Xie, H. Mao, L. Tan, Y. Zhang and Y. Chen, *Adv. Funct. Mater.*, 2021, **31**, 2102291.
54 X. Wang, Q. Sun, J. Gao, J. Wang, C. Xu, X. Ma and F. Zhang, *Energies*, 2021, **14**, 4200.
55 G. Zhang, H. Ning, H. Chen, Q. Jiang, J. Jiang, P. Han, L. Dang, M. Xu, M. Shao, F. He and Q. Wu, *Joule*, 2021, **5**, 931–944.
56 K. Yang, Z. Zhao, M. Liu, Z. Zhou, K. Wang, X. Ma, J. Wang, Z. He and F. Zhang, *Chem. Eng. J.*, 2022, **427**, 131802.
57 L. Huang, P. Jiang, Y. Zhang, L. Zhang, Z. Yu, Q. He, W. Zhou, L. Tan and Y. Chen, *ACS Appl. Mater. Interfaces*, 2019, **11**, 26213–26221.
58 C. Xu, Z. Zhao, K. Yang, L. Niu, X. Ma, Z. Zhou, X. Zhang and F. Zhang, *J. Mater. Chem. A*, 2022, DOI: 10.1039/D1TA10581G.